



The role of shallow convection in promoting the northward propagation of boreal summer intraseasonal oscillation

Fei Liu¹ · Jiuwei Zhao¹ · Xiuhua Fu² · Gang Huang^{3,4}

Received: 14 January 2016 / Accepted: 26 January 2017 / Published online: 4 February 2017
© Springer-Verlag Wien 2017

Abstract By conducting idealized experiments in a general circulation model (GCM) and in a toy theoretical model, we test the hypothesis that shallow convection (SC) is responsible for explaining why the boreal summer intraseasonal oscillation (BSISO) prefers propagating northward. Two simulations are performed using ECHAM4, with the control run using a standard detrainment rate of SC and the sensitivity run turning off the detrainment rate of SC. These two simulations display dramatically different BSISO characteristics. The control run simulates the realistic northward propagation (NP) of the BSISO, while the sensitivity run with little SC only simulates stationary signals. In the sensitivity run, the meridional asymmetries of vorticity and humidity fields are simulated under the monsoon vertical wind shear (VWS); thus, the frictional convergence can be excited to the north of the BSISO. However, the lack of SC makes the lower and middle troposphere very dry, which prohibits further development of deeper convection. A theoretical BSISO model is also constructed, and the result shows that SC is a key to convey the asymmetric vorticity effect to induce the BSISO to move northward. Thus, both the GCM and theoretical model results demonstrate the importance of SC in promoting the NP of the BSISO.

✉ Gang Huang
hg@mail.iap.ac.cn

¹ Earth System Modeling Center and climate dynamics research center, Nanjing University of Information Science and Technology, Nanjing, China

² International Pacific Research Center and Department of Meteorology, University of Hawaii at Manoa, Honolulu, HI, USA

³ State Key Laboratory of Numerical Modeling for Atmospheric Sciences and Geophysical Fluid Dynamics, Institute of Atmospheric Physics, Chinese Academy of Sciences, Beijing 100029, China

⁴ University of Chinese Academy of Sciences, Beijing 100049, China

1 Introduction

The Indian summer monsoon (ISM) always experiences a dominant 20–50-day oscillation, which is controlled by the boreal summer intraseasonal oscillation (BSISO) (Krishnamurti and Bhalme 1976; Gadgil 2003). Along with strong self-induced oscillation in the ISM (Liu and Wang 2012a, 2014), the northward propagation (NP) of BSISO is demonstrated to be responsible for these wet and dry events of the ISM (Annamalai and Slingo 2001). The BSISO over the western North Pacific, which is often modulated by El Niño/Southern Oscillation (ENSO) (Liu et al. 2016), also can contribute to the intraseasonal variation in the East Asian monsoon. Although the BSISO has attracted many years of studying, current climate model still suffers low ability of BSISO simulation (Lin et al. 2008).

To improve the BSISO simulation, a large amount of previous works try to explain why the BSISO prefers moving poleward. Internal atmospheric dynamic processes have been well studied to understand the BSISO. In the first time, Lau and Peng (1990) demonstrated the role of the equatorial Rossby waves in monsoon NP, which is triggered by the interaction between the monsoon mean flows and the Madden-Julian oscillation (MJO). The NP of the BSISO can also be caused by the Rossby wave emanation, which tends to form the northwestward slanted rain band (Wang and Xie 1997). The general circulation model (GCM) simulations also confirm this result (Wu et al. 2006). In one landmark study, the barotropic vorticity (BV) generated by baroclinic-barotropic interaction under the easterly vertical wind shear (VWS) was found to be important for the independent poleward migrating event of the BSISO (Jiang et al. 2004). This north-of-convection BV was also found to be generated by vertical

transport of monsoon mean winds (Drbohlav and Wang 2005), by poleward transport of anomalous vorticity (Bellon and Sobel 2008), and by cumulus momentum transport (Liu et al. 2015). By using a cloud-resolving model, the NP of the BSISO was also generated by the beta drift near the equator, in which the planetary boundary layer (PBL) will interact with these drifting gyres and enhance the low-tropospheric moisture (Boos and Kuang 2010). In the GCM simulations, the cumulus momentum transport was also found to be the key process to control the NP of the BSISO (Kang et al. 2010).

Apart from the internal atmospheric processes, external surface heat fluxes were also found to contribute to the poleward migration of the BSISO. Existences of meridional gradients in seasonal-mean moist static energy and surface heat flux were found to favor the NP of the BSISO (Webster 1983; Gyoswami and Shukla 1984). Atmosphere-ocean interaction was also shown to contribute to the NP, because warm sea surface temperature (SST) will be favorable for the growing of new convection in the poleward of the original rain band, resulting in the NP of BSISO (Fu et al. 2003; Sperber and Annamalai 2008).

Although affected by external forcing, the BSISO has been known as an internal mode in the tropical atmosphere (Madden and Julian 1994; Wang 2005; Ajayamohan et al. 2011). The PBL moisture transport and the role of BV were found to be keys for inducing the poleward propagation of the BSISO, as well as the BV effect (DeMott et al. 2013). Based on recent high-resolution observations, the shallow convection (SC) has been found to prevail leading the BSISO convection to the north (Abhik et al. 2013). The SC is favorable for preconditioning the atmosphere for deep convection, and the BSISO tilts backward against its NP (Abhik et al. 2013). Based on the satellite and reanalysis data (Stephens et al. 2002; Simmons et al. 2007), this dominant vertical-tilted profile has also been found in the cloud water for the poleward-propagating BSISO (Jiang et al. 2011). The multi-cloud structure, consisted of low-level shallow congestus, deep convection, and upper-level stratiform, was discovered for the BSISO. These observations should suggest that the SC should be important in the NP of the BSISO.

Considering the importance of SC in simulating the boreal winter MJO by using the atmospheric GCM (Zhang and Song 2009), this paper focuses on the role of SC in the BSISO simulated by ECHAM4 AGCM. We also use a theoretical BSISO skeleton model to explain the AGCM results.

In Section 2, the observational data, the atmospheric GCM simulations, and the theoretical model for the BSISO are discussed. In Section 3, the model results are presented. Experiments based on the toy theoretical model are reported in Section 4. The last section will summarize the paper.

2 Models and data

2.1 Data

Monthly mean winds and specific humidity used in this paper are obtained from the NCEP Reanalysis II (Kanamitsu et al. 2002). The high-frequency Tropical Rainfall Measuring Mission (TRMM) 3B42 precipitation is also analyzed to obtain the BSISO signal for the period of 1998–2012 (Huffman et al. 2007). To isolate the intraseasonal signal, the 20–100-day band-pass filter is performed on each meteorological field.

2.2 GCM experiments

To simulate the BSISO, we employ the ECHAM version 4 (ECHAM4) that has a good simulation of BSISO (Jiang et al. 2004). In this study, a coarse resolution of T30 for horizontal direction and 19 vertical levels are used. The modified Tiedtke convection scheme is used (Nordeng 1994). Previous works have shown a good simulation of NP of the BSISO by using the ECHAM4 (Fu et al. 2003; Jiang et al. 2004). Two dominant mechanisms, i.e., the BV effect (Jiang et al. 2004) and the air-sea interaction effect (Fu et al. 2003) for the NP of the BSISO, can be well captured by ECHAM4. Thus, we still use this old version of ECHAM. In order to explore how the SC works in the BSISO, two simulations are carried out in this study. In the first experiment, referred to as CTL (for control), the standard ECHAM4 is used. This is the same simulation as that used by Jiang and his colleagues (Jiang et al. 2004). In the second experiment, referred to as Exp WS (for weak SC), the detrainment of cloud water from SC is turned off. After the spin up, we run this model for 15 years for each case. In these two case runs, the boundary forcing is the same by using climatological monthly mean SST for the period of 1990–2010.

2.3 A theoretical model for the BSISO

To understand the role of SC, we use a two-and-a-half-layer model that was designed to study the BSISO (Liu et al. 2015). This model is originally built for the neutral MJO skeleton (Majda and Stechmann 2009) and developed by Liu and Wang (2012b) for the unstable eastward moving MJO. This model includes the dominant mechanisms for the MJO, the wave, and the moisture feedbacks (Liu and Wang 2016a, 2016b). In order to describe the moisture process, we consider the full moisture equation. The moisture anomalies, neglected in the wave dynamics, have been added. The precipitation has been parameterized based on the observation that the positive moisture anomaly tends to enhance the precipitation (Majda and Stechmann 2009).

Cumulus convection has been found to be very sufficient to mix the VWS (Wu and Yanai 1994); thus, cumulus

momentum transport is included in this model. In this skeleton model, the BV induced by cumulus momentum transport will produce strong moisture convergence in the PBL in the front of the BSISO rain band, which should induce the NP of the BSISO (DeMott et al. 2013). In this theoretical model, the effect of the cumulus convection is parameterized following the work of Schneider and Lindzen (1976); we assume that the barotropic cumulus momentum transport is proportional to the anomalous vertical velocity and the monsoon VWS. In the monsoon region which has a strong easterly VWS, the anomalous upward wind in the positive phase of the BSISO tends to enhance the barotropic westerly wind anomalies, while the anomalous downward wind anomalies will enhance the easterly winds.

Observational studies have demonstrated the role of SC, which tends to moisten the low-level atmosphere in front of the ISO through the positive moisture convergence in the PBL (Hendon and Salby 1994). To mimic the role of SC, we assume that the moisture anomaly is proportional to the positive moisture convergence in the PBL in the moisture equation, as did in the frictional skeleton model (Liu and Wang 2012b). Thus, deep convection can be enhanced by the moist lower troposphere in this simple model.

The temporal and spatial scales are represented by $[T] = (C\beta)^{-1/2}$ and $[L] = (C/\beta)^{1/2}$ where $\beta = 2.29 \times 10^{-11} \text{ m}^3 \text{s}^{-1}$ is the equatorial curvature effect of the earth for the first order and $C = (gH)^{1/2}, 50 \text{ ms}^{-1}$ is the gravity wave velocity. The non-dimensionalized equations for the model are expressed as follows,

$$\begin{aligned} \partial_t u_- - yv_- - \partial_x T_- &= -du_-, \\ yu_- - \partial_y T_- &= 0, \\ \partial_t T_- - \partial_x u_- - \partial_y v_- &= P - dT_-, \\ \partial_t q_- + \tilde{Q}(\partial_x u_- + \partial_y v_-) &= -P + r_b(T_s - 9.18)w_b, \\ \partial_t P &= \Gamma q_-, \\ \partial_t u_+ - yv_+ - \partial_x T_+ &= CMT - du_+, \\ yu_+ - \partial_y T_+ &= 0, \\ \partial_x u_+ + \partial_y v_+ + w_b &= 0, \\ w_b &= -(d_1 \nabla^2 + d_2 \partial_x + d_3 \partial_y)(T_- + T_+), \end{aligned} \quad (1)$$

where u and v are the horizontal velocities, T is the temperature, P is the diabatic heating associated with deep convection, and q is the moisture anomaly. w_b is the Ekman pumping in the PBL, and CMT is the barotropic cumulus momentum transport. Subscript “−” denotes the baroclinic mode, subscript “+” denotes the barotropic mode, and subscript “b” stands for the PBL.

In this model, the same value of d has been used for the Rayleigh friction and Newtonian cooling. \tilde{Q} demonstrates the vertical profile of mean humidity in the troposphere. Γ is a precipitation coefficient measuring how strongly the precipitation responds to the anomalous moisture.

r_b is a PBL coefficient that represents the efficiency of moisture transfer from the PBL to the lower troposphere caused by SC. Large r_b means strong SC that moistens the lower troposphere. The PBL coefficients are $d_1 = H_b E / H_T(E^2 + y^2)$, $d_2 = -H_b(E^2 - y^2)/H_T(E^2 + y^2)$, and $d_3 = -2H_b E y / H_T(E^2 + y^2)^2$, where H_b is the PBL depth, H_T is the tropospheric depth, and E measures the PBL friction. The barotropic cumulus momentum transport is measured by the anomalous precipitation P and seasonal-mean VWS U . This transport can be parameterized as $\text{CMT} = -sUP$, where s is the cumulus momentum transport coefficient, which measures how strong the momentum transport will be excited by the anomalous vertical motions. U is the background easterly VWS. T_s is the zonally averaged SST. More details of these parameters are referred to Table 1.

3 GCM results with strong and weak SCs

Figure 1a–c shows the climatological precipitation and VWS of the boreal summer (June–September) for these 15 years. VWS is defined as the difference of zonal winds between the upper (200 hPa) and lower (850 hPa) troposphere in both observation and model simulations. Compared to the observation (Fig. 1a), the dominant precipitation distribution has been simulated by the CTL, for example, the simulated precipitation centers in the western North Pacific as well as in the equatorial Indian Ocean agree with the observations well, although the model overestimates the precipitation in the Indian Ocean. A large bias in the rainfall has also been simulated in the Bay of Bengal region. Exp WS has strong precipitation to the south of the equator and over the Bay of Bengal. The seasonal-mean easterly VWS, an essential factor for exciting the BV by barotropic-baroclinic interaction (Jiang et al. 2004) or by cumulus momentum transport (Liu et al. 2015), is well simulated over the Bay of Bengal. Figure 1d–f compares the observed and simulated BSISO propagation over the Bay of Bengal in these two runs. By defining the BSISO index as the box (2.5° – 7.5° N, 85° – 95° E) averaged 20–100 day filtered precipitation, the propagation can be calculated through the lead-lag correlation for the 85° – 95° E latitude belt. In the observation, significant NP is present (Fig. 1d). In CTL (Fig. 1e), anomalous convection also shows significant NP with a speed of about $0.9^\circ \text{ day}^{-1}$. The NP, however, disappears in Exp WS; instead, it shows a stationary mode (Fig. 1f).

Figure 2 displays the meridional-vertical distributions of climatological specific humidity for both the observation and simulations. During the boreal summer, the Bay of Bengal has more moisture than the equatorial Indian Ocean in the observation (Fig. 2a), and the CTL simulation well captures this northward gradient of seasonal-mean moisture (Fig. 2b). In Exp WS with the SC suppressed (Fig. 2c), although this northward gradient can be

Table 1 Parameters and their standard values used in the theoretical model

Parameter	Description	Typical value utilized here (non-dimensional)
d	Tropospheric damping coefficient	0.07 (1/5 day)
\tilde{Q}	Vertical gradient of background moisture in lower troposphere	0.9 (7.3 g kg^{-1})
T_{s0}	Magnitude of the sea surface temperature	29 °C
Γ	Precipitation coefficient	0.018 ($0.2 \text{ K}^{-1} \text{ day}^{-1}$)
r_b	Coefficient of moisture transfer by SC	0.06
s	Cumulus momentum transport coefficient	1.25 (0.5 cm^{-1})
U_0	Magnitude of background VWS	0.2 (20 ms^{-1})
E	Ekman number in the PBL	1.1 (1/8 h)
H_b	PBL depth	1 km
H_T	Lower-tropospheric depth	5.1 km

simulated, the simulated lower-tropospheric atmosphere is much drier than that in the observation and in the Exp CTL. Since the atmospheric column cannot be moistened due to the lack of moistening process of SC, all kinds of convection, from the seasonal mean (Fig. 2c) to the intraseasonal and synoptic scales (figure not shown), are weak in Exp WS.

Figure 3 gives the meridional-vertical section of the regressed northward propagation in Exp CTL and the

stationary oscillation in Exp WS. In the Exp CTL (Fig. 3a–d), the maximum clouds are simulated in the mid troposphere (near 300 hPa), which is consistent with the simulated convective center. Because of the convection, lower-tropospheric convergence and up-level divergence have been simulated. A significant asymmetry has been simulated in the vorticity and specific humidity. Strong BV anomalies have been found to lead the convective center to the north by a phase of 6° (Fig. 3c). Such BV

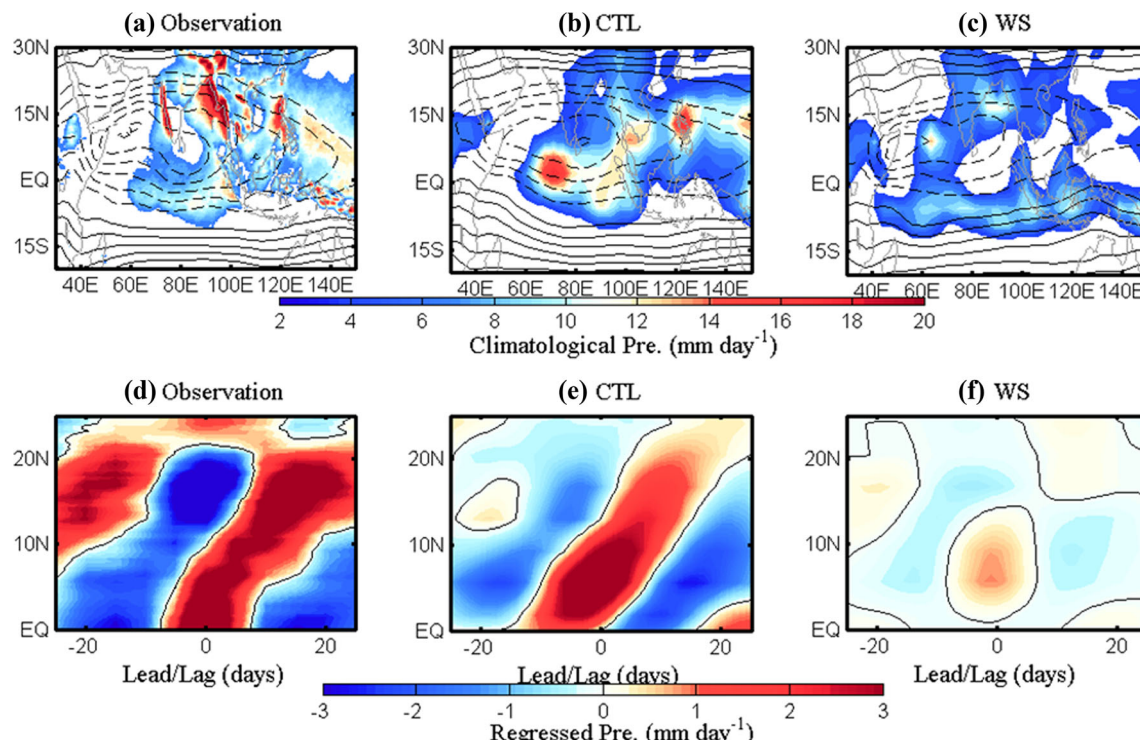


Fig. 1 Top: June–September averaged climatological precipitation (mm day^{-1} , shading) and vertical wind shear (m s^{-1} , contour) defined by $U_{200\text{hPa}}$ minus $U_{850\text{hPa}}$ from **a** observation, **b** CTL, and **c** Exp WS. The observational precipitation and wind are obtained from TRMM and NCEP Reanalysis II. Contour interval is 5 m s^{-1} and zero contours are not drawn. Positive and negative values are denoted by solid and dashed

lines. Bottom: latitude-lag regression plots against the BSISO index using longitude (85° – 95° E) averages of precipitation anomalies (mm day^{-1} , shading) with time scales of 20–100 days from **d** observation, **e** CTL, and **f** Exp WS. Thin black contour represents zero. The BSISO index is defined by the box-averaged (2.5° – 7.5° N, 85° – 95° E) precipitation anomalies with time scales of 20–100 days

Fig. 2 Height-latitude cross section of June–September averaged climatological specific humidity (g kg^{-1} , shading) averaged over $85^{\circ}\text{--}95^{\circ}$ E from **a** observation (NCEP Reanalysis II), **b** CTL, and **c** Exp WS

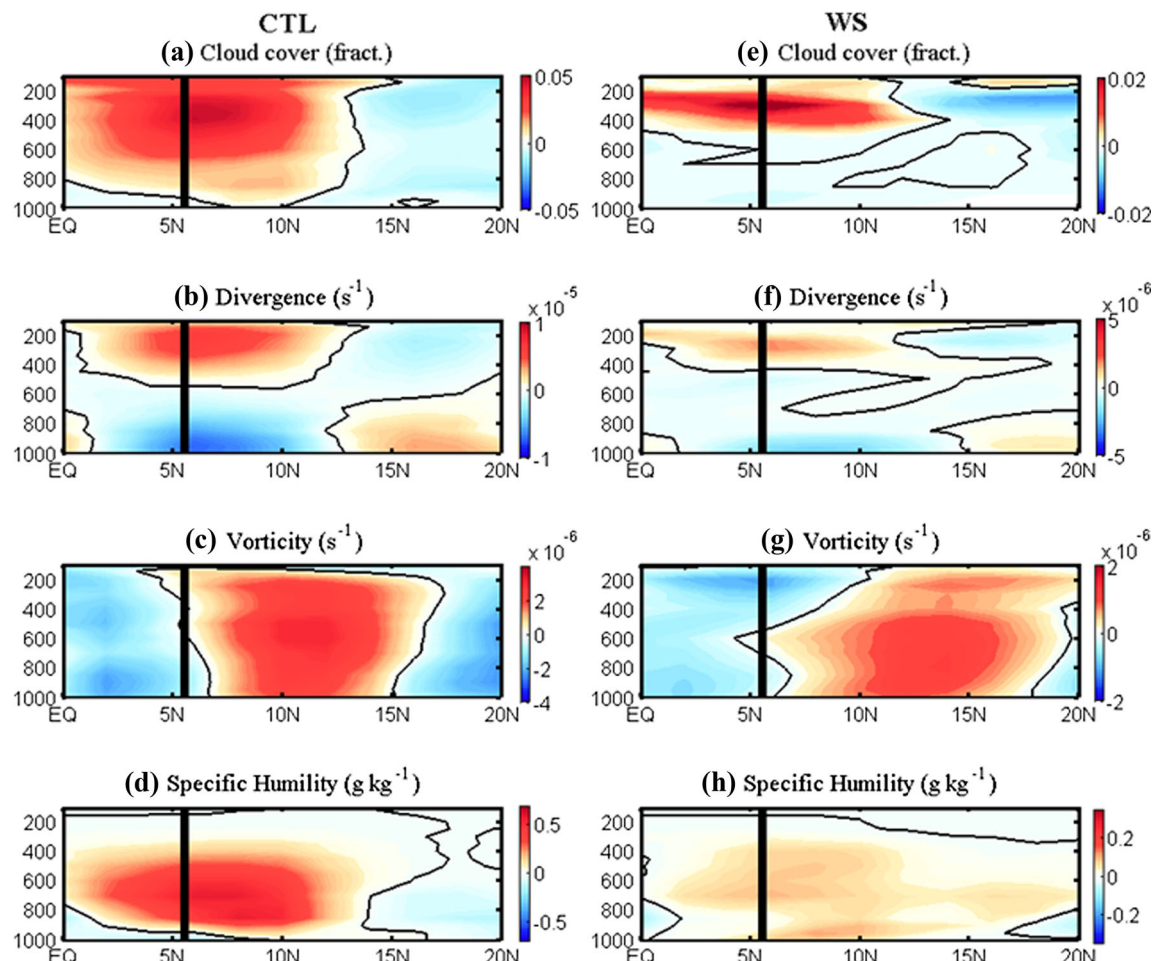
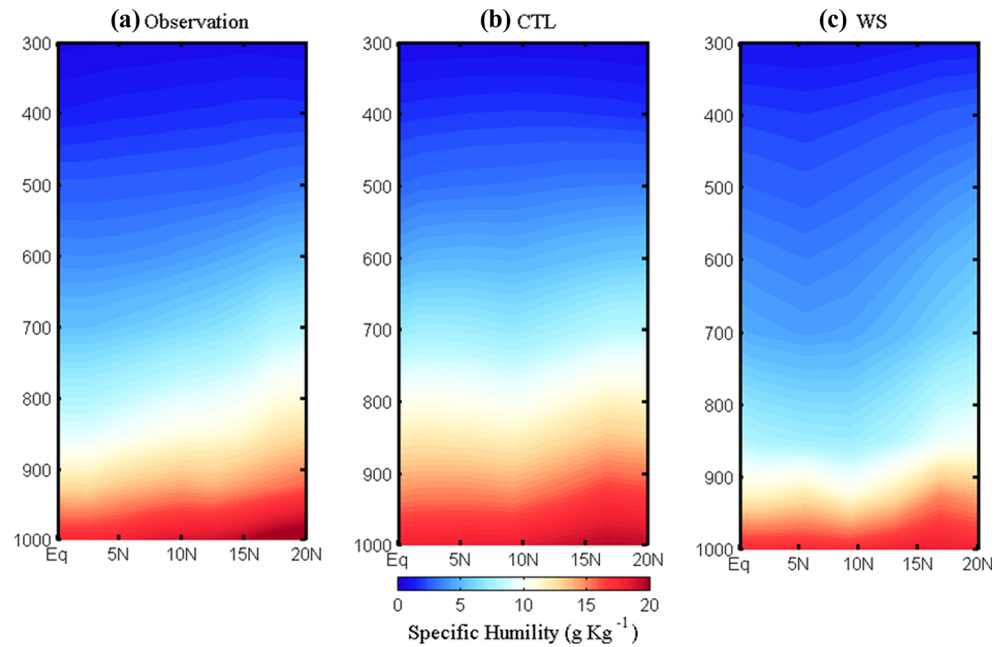
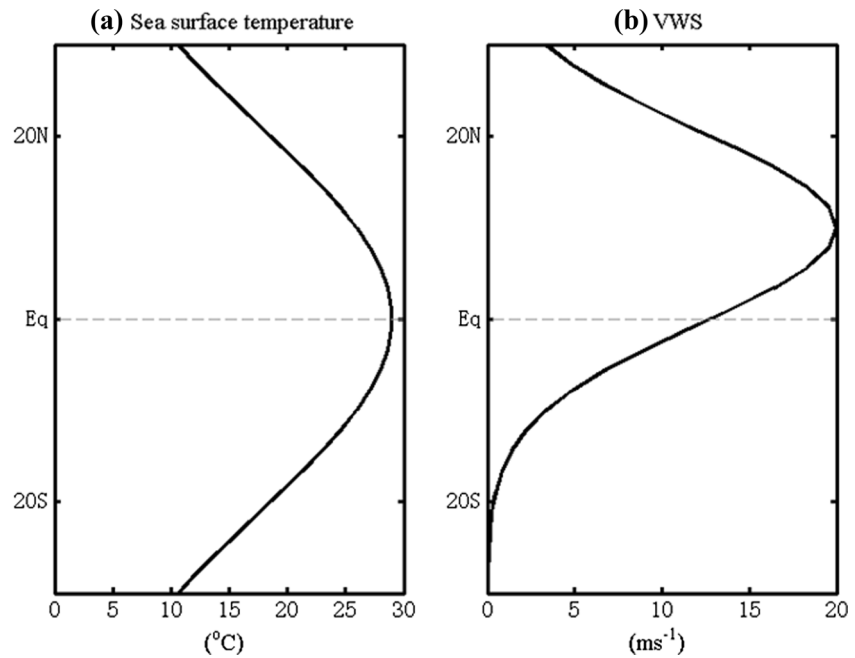


Fig. 3 Regressed meridional-vertical structure averaged over $85^{\circ}\text{--}95^{\circ}$ E against the BSISO index in CTL and Exp WS: **a, e** cloud cover (fract.); **b, f** divergence (s^{-1}); **c, g** vorticity (s^{-1}); and **d, h** specific humidity (g kg^{-1})

The horizontal axis is latitude, and the vertical axis is pressure (hPa). Thick black vertical line denotes the convective center where maximum precipitation occurs, and thin black contour represents zero

Fig. 4 Meridional distributions of zonal-mean **a** SST ($^{\circ}\text{C}$) and **b** VWS (m s^{-1}) used in the theoretical model



anomalies tend to produce the moisture convergence in the PBL. The SC is also found to be increased in the front of the convective center, which prefers moistening the lower troposphere, resulting in the NP of the convection (Fig. 3d).

Figure 3e–h shows the results from Exp WS, in which the cloud is suppressed in the lower troposphere and the SC is much prohibited due to the lack of detrainment for SC. The significant asymmetric structure has also been simulated for the vorticity and PBL convergence in Exp WS. In front of the convective center, the BV as well as the PBL moisture convergence has been excited. The moisture, however, cannot be transported to the lower troposphere due to the lack of strong SC. The dry lower and mid troposphere prohibits the triggering of deep convection; thus, no NP can be induced.

4 Theoretical model results

In this section, we tend to explore the role of SC through a theoretical model developed by Liu et al. (2015). Assuming that the background easterly VWS U is centered at 10°N and has a meridional damping scale of 15° (Fig. 4a) centered, thus, it can be represented as $U = U_0 \exp(-((y - 0.75)/1.1)^2)$. The zonally averaged SST is assumed to have a meridional structure of $T_{s0} \exp(-(y/2.3)^2)$, which maxima are centered on the equator and also have a poleward damping scale of 30° (Fig. 4b).

To study the role of SC, two experiments are carried out using $r_b = 0.06 \text{ K}^{-1}$ (for strong SC, Exp SSC) and $r_b = 0.006 \text{ K}^{-1}$ (for weak SC, Exp WSC). The experiments use the same initial baroclinic wavenumber-one disturbances,

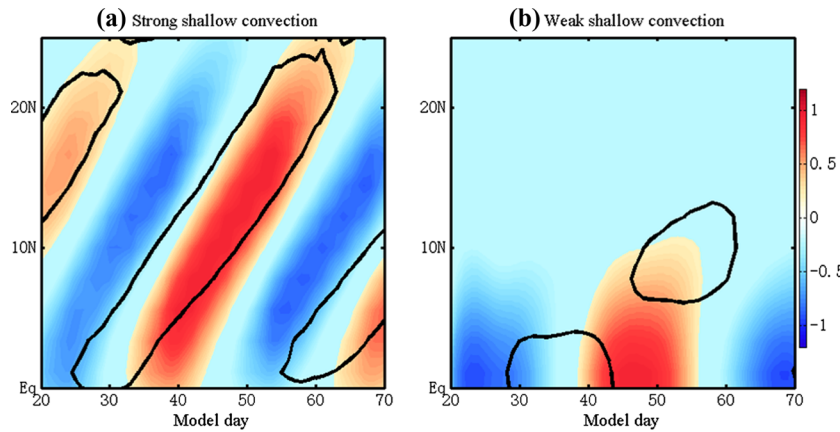
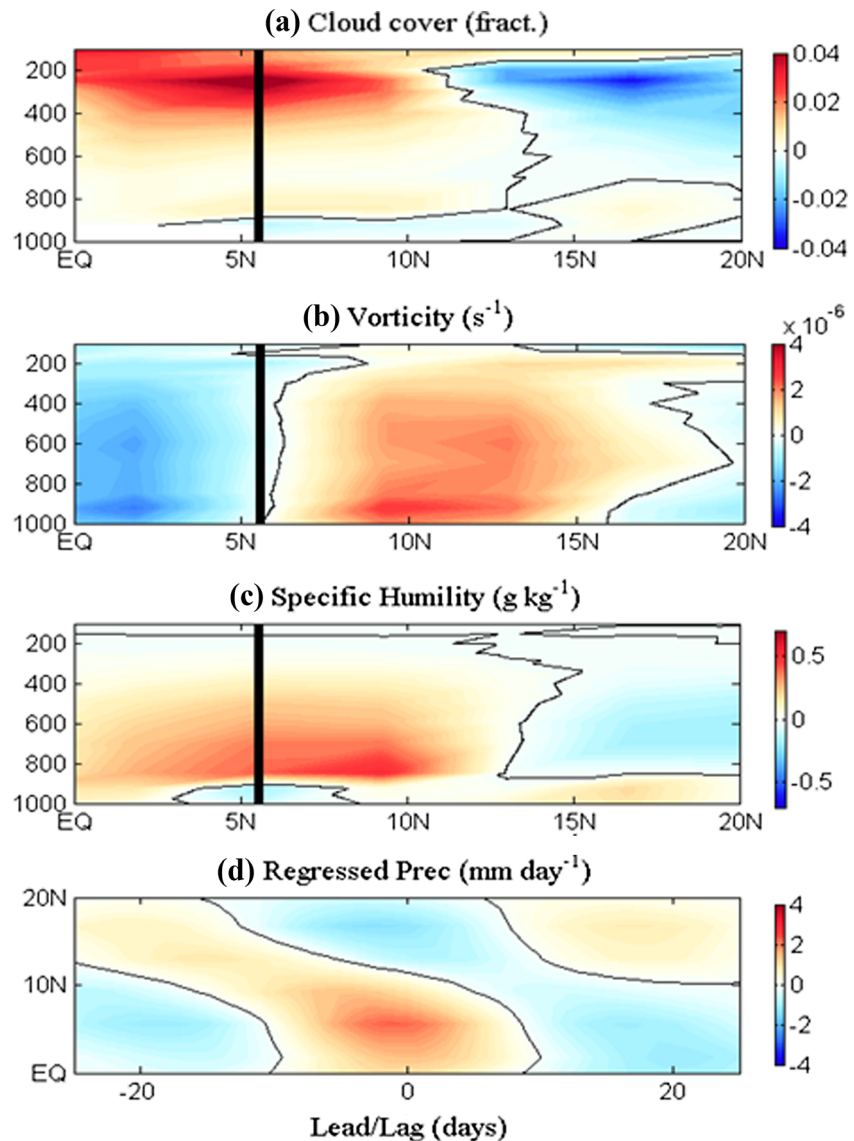


Fig. 5 Hovmöller plots of precipitation anomalies (shading) averaged over 85° – 95°E from day 20 through day 70 for different experiments of the theoretical model: **a** strong SC (SSC) $r_b = 0.06 \text{ K}^{-1}$ and **b** weak SC (WSC) $r_b = 0.006 \text{ K}^{-1}$. Black contours denote upward Ekman pumping

that has a value of one third of its magnitude. The x -axis shows model days, and the y -axis, latitude. Global precipitation and Ekman pumping are normalized by their maximum values on each day

Fig. 6 Regressed meridional-vertical structure averaged over 85°–95° E against the BSISO index in Exp WD: **a** cloud cover (fract.), **b** vorticity (s^{-1}), and **c** specific humidity ($g kg^{-1}$). The horizontal axis is latitude, and the vertical axis is pressure (hPa). Thick black vertical line denotes the convective center. **d** Latitude-lag regression plot using the longitude average of 85°–95° E for precipitation anomalies ($mm day^{-1}$) with time scales of 20–100 days. Thin black contour represents zero



which have the maxima at the equator with a meridional damping scale of 30°. We integrate the model using the finite difference method.

Figure 5 shows the model evolution in the two experiments. In Exp SSC, a robust NP is simulated (Fig. 5a). The simulated BSISO shows a NP speed of 0.77°/day, which is consistent with the observed value of 0.75°/day over the Bay of Bengal (Kang et al. 2010). The cumulus momentum transport, accelerating the barotropic westerly (easterly) wind when the precipitation anomalies are positive (negative), excites a dipole-like barotropic wind tendency in the meridional direction, resulting in BV anomalies in front of the precipitation center; thus, the moisture convergence is excited in the PBL by this vorticity forcing. Because of the strong SC, the moisture convergence in the PBL prefers moistening the atmosphere and induces the NP by enhancing the deep convection.

When the SC is much suppressed in Exp WSC, the NP disappears (Fig. 5b). The cumulus momentum transport still accelerates the barotropic zonal velocity and excites the BV which leads the convective center to the north. Although the resulting upward Ekman pumping can be excited, the dry lower troposphere, however, is still caused, since the moisture cannot be transported upward in front of the convective center. This means that the deep convection cannot be triggered to induce the NP. This result confirms that SC is essential for conveying the asymmetric vorticity effect to induce the NP of the BSISO.

Since this theoretical model is a linear system, the role of SC can be easily included or removed by a coefficient setting. The theoretical model presents a clear figure showing how the SC affects the NP of the BSISO. In the GCM, the PBL effect is always included, and why the poleward movement of the BSISO is suppressed when turning off the SC? From the

analysis of this linear theoretical model, we can see the reason is that the PBL effect and the tropospheric circulation are not coupled without the SC.

In this toy model, only the convective momentum transport is included to induce the asymmetric BV for the poleward movement of the BSISO. Another important “VWS mechanism,” or baroclinic-barotropic interaction within the monsoon VWS responsible for this NP (Jiang et al. 2004), is neglected. Relative roles of these two mechanisms in producing the asymmetric BV need to be investigated through observation analysis, model simulation and theoretical analysis.

5 Discussion

We investigate the roles of SC in the BSISO simulations using a GCM of ECHAM4 and the theoretical BSISO model. It is shown that both complex GCM and simple theoretical model can simulate the NP of the BSISO, only when they include strong SC. These results confirm that the SC is critical for the NP of the BSISO, as shown in the observational study of Abhik et al. (2013). Within the monsoon region, the BV can be excited to lead the convection to the north through cumulus momentum transport (Liu et al. 2015) or by barotropic-baroclinic interaction (Jiang et al. 2004). Such BV can also excite PBL convergence. However, it is the SC that acts to convey this asymmetric structure to induce the NP of the BSISO. Even with this asymmetric vorticity structure, the lower troposphere, however, can only be moistened when the SC is presented; otherwise no NP of deep convection would appear. Although plenty of previous works have demonstrated the importance of BV in inducing the NP of the BSISO under the monsoon easterly VWS (Jiang et al. 2004), our new finding shows that the SC is the key to transfer this BV effect to the NP of the BSISO by coupling the tropospheric circulation and PBL moisture convergence. Recent works also show that the longwave radiation is important for the MJO (Chikira 2014; Kim et al. 2015), and the longwave radiation effect on the BSISO can also be studied through another sensitivity experiment by turning off the longwave radiation in future works.

Considering the importance of SC in the MJO simulation (Zhang and Song 2009), SC is shown to be indispensable for simulating the NP of the BSISO. There is no doubt that deep convection is critical to simulate the NP of the BSISO. An experiment, referred to as Exp WD (for weak deep convection), is carried out using ECHAM4, which is the same as Exp WS except using default SC detrainment and turning off penetrative convection detrainment. This experiment simulates a weak equatorward propagation (Fig. 6). Although the asymmetric BV can be excited to the north of the convective center, as well as sufficient moisture transport to the lower troposphere, the deep convection is largely suppressed by the lack

of detrainment of penetrative convection; so, the NP cannot be simulated. A good simulation of multi-cloud interaction is a key to the BSISO simulation.

Acknowledgements This work was supported by the National Natural Science Foundation of China (41275083, 91337105, 41425019 and 41420104002), the China National 973 Project (2015CB453200), the Natural Science Foundation of Jiangsu (BK20150907), and the public science and technology research funds projects of ocean (201505013). This paper is ESMC Contribution No. 146.

References

- Abhik S, Halder M, Mukhopadhyay P, Jiang X, Goswami B (2013) A possible new mechanism for northward propagation of boreal summer intraseasonal oscillations based on TRMM and MERRA reanalysis. *Clim Dynam* 40:1611–1624
- Ajayamohan R, Annamalai H, Luo J-J, Hafner J, Yamagata T (2011) Poleward propagation of boreal summer intraseasonal oscillations in a coupled model: role of internal processes. *Clim Dynam* 37:851–867
- Annamalai H, Slingo J (2001) Active/break cycles: diagnosis of the intraseasonal variability of the Asian summer monsoon. *Clim Dynam* 18:85–102
- Bellon G, Sobel AH (2008) Instability of the axisymmetric monsoon flow and intraseasonal oscillation. *Journal of Geophysical Research: Atmospheres* 1984–2012:113
- Boos WR, Kuang Z (2010) Mechanisms of poleward propagating, intraseasonal convective anomalies in cloud system-resolving models. *J Atmos Sci* 67:3673–3691
- Chikira M (2014) Eastward-propagating intraseasonal oscillation represented by Chikira–Sugiyama cumulus parameterization. Part II: understanding moisture variation under weak temperature gradient balance. *J Atmos Sci* 71:615–639
- DeMott CA, Stan C, Randall DA (2013) Northward propagation mechanisms of the boreal summer intraseasonal oscillation in the ERA-Interim and SP-CCSM. *J Clim* 26:1973–1992
- Drbohlav H-KL, Wang B (2005) Mechanism of the northward-propagating intraseasonal oscillation: insights from a zonally symmetric model*. *J Clim* 18:952–972
- Fu X, Wang B, Li T, McCreary JP (2003) Coupling between northward-propagating, intraseasonal oscillations and sea surface temperature in the Indian Ocean*. *J Atmos Sci* 60:1733–1753
- Gadgil S (2003) The Indian monsoon and its variability. *Annu Rev Earth Pl Sc* 31:429–467
- Goswami B, Shukla J (1984) Quasi-periodic oscillations in a symmetric general circulation model. *J Atmos Sci* 41:20–37
- Hendon HH, Salby ML (1994) The life cycle of the Madden-Julian oscillation. *J Atmos Sci* 51:2225–2237
- Huffman GJ, Bolvin DT, Nelkin EJ, Wolff DB, Adler RF, Gu G, Hong Y, Bowman KP, Stocker EF (2007) The TRMM multisatellite precipitation analysis (TMPA): quasi-global, multiyear, combined-sensor precipitation estimates at fine scales. *J Hydrometeorol* 8:38–55
- Jiang X, Li T, Wang B (2004) Structures and mechanisms of the northward propagating boreal summer intraseasonal oscillation*. *J Clim* 17:1022–1039
- Jiang X, Waliser DE, Li J-L, Woods C (2011) Vertical cloud structures of the boreal summer intraseasonal variability based on CloudSat observations and ERA-Interim reanalysis. *Clim Dynam* 36:2219–2232
- Kanamitsu M, Ebisuzaki W, Woollen J, Yang S-K, Hnilo J, Fiorino M, Potter G (2002) NCEP-DOE AMIP-II reanalysis (R-2). *Bull Am Meteorol Soc* 83:1631–1643

- Kang I-S, Kim D, Kug J-S (2010) Mechanism for northward propagation of boreal summer intraseasonal oscillation: convective momentum transport. *Geophys Res Lett* 37:24804
- Kim D, Ahn M-S, Kang I-S, Del Genio AD (2015) Role of longwave cloud–radiation feedback in the simulation of the Madden–Julian oscillation. *J Clim* 28:6979–6994
- Krishnamurti TN, Bhalme H (1976) Oscillations of a monsoon system. Part I. Observational aspects. *J Atmos Sci* 33:1937–1954
- Lau K, Peng L (1990) Origin of low frequency (intraseasonal) oscillations in the tropical atmosphere part III: monsoon dynamics. *J Atmos Sci* 47:1443–1462
- Lin J-L, Weickman KM, Kiladis GN, Mapes BE, Schubert SD, Suarez MJ, Bacmeister JT, Lee M-I (2008) Subseasonal variability associated with Asian summer monsoon simulated by 14 IPCC AR4 coupled GCMs. *J Clim* 21:4541–4567
- Liu F, Wang B (2012a) A conceptual model for self-sustained active-break Indian summer monsoon. *Geophys Res Lett* 39:L20814
- Liu F, Wang B (2012b) A frictional skeleton model for the Madden–Julian oscillation. *J Atmos Sci* 69:2749–2758
- Liu F, Wang B (2014) A mechanism for explaining the maximum intraseasonal oscillation center over the Western North Pacific*. *J Clim* 27:958–968
- Liu F, Wang B (2016a) Effects of moisture feedback in a frictional coupled Kelvin–Rossby wave model and implication in the Madden–Julian oscillation dynamics. *Clim Dynam*:DOI:[10.1007/s00382-00016-03090-y](https://doi.org/10.1007/s00382-00016-03090-y)
- Liu F, Wang B (2016b) Role of horizontal advection of seasonal-mean moisture in the Madden–Julian oscillation: a theoretical model analysis. *J Climate*:DOI:[10.1175/JCLI-D-1116-0078.1171](https://doi.org/10.1175/JCLI-D-1116-0078.1171).
- Liu F, Wang B, Kang I-S (2015) Roles of barotropic convective momentum transport in the intraseasonal oscillation. *J Clim* 28:4908–4920
- Liu F, Li T, Wang H, Deng L, Zhang Y (2016) Modulation of boreal summer intraseasonal oscillations over the western North Pacific by ENSO. *J Climate*:DOI:[10.1175/JCLI-D-1115-0831.1171](https://doi.org/10.1175/JCLI-D-1115-0831.1171).
- Madden RA, Julian PR (1994) Observations of the 40–50-day tropical oscillation—a review. *Mon Weather Rev* 122:814–837
- Majda AJ, Stechmann SN (2009) The skeleton of tropical intraseasonal oscillations. *Proc Natl Acad Sci U S A* 106:8417–8422
- Nordeng TE (1994) Extended versions of the convective parametrization scheme at ECMWF and their impact on the mean and transient activity of the model in the tropics. European Centre for Medium-Range Weather Forecasts
- Schneider EK, Lindzen RS (1976) A discussion of the parameterization of momentum exchange by cumulus convection. *J Geophys Res* 81: 3158–3160
- Simmons A, Uppala S, Dee D, Kobayashi S (2007) ERA-Interim: new ECMWF reanalysis products from 1989 onwards. *ECMWF Newslett* 110:25–35
- Sperber KR, Annamalai H (2008) Coupled model simulations of boreal summer intraseasonal (30–50 day) variability, part 1: systematic errors and caution on use of metrics. *Clim Dynam* 31:345–372
- Stephens GL, Vane DG, Boain RJ, Mace GG, Sassen K, Wang Z, Illingworth AJ, O'Connor EJ, Rossow WB, Durden SL (2002) The CloudSat mission and the A-Train: a new dimension of space-based observations of clouds and precipitation. *Bull Am Meteorol Soc* 83:1771–1790
- Wang B (2005) Theories. In: Lau, K.-M., Waliser, D.E. (Eds.), *Intraseasonal variability of the atmosphere-ocean climate system*. Springer-Verlag, Heidelberg, Germany
- Wang B, Xie X (1997) A model for the boreal summer intraseasonal oscillation. *J Atmos Sci* 54:72–86
- Webster PJ (1983) Mechanisms of monsoon low-frequency variability: surface hydrological effects. *J Atmos Sci* 40:2110–2124
- Wu X, Yanai M (1994) Effects of vertical wind shear on the cumulus transport of momentum: observations and parameterization. *J Atmos Sci* 51:1640–1660
- Wu M-LC, Schubert SD, Suarez MJ, Piegion PJ, Waliser DE (2006) Seasonality and meridional propagation of the MJO. *J Clim* 19: 1901–1921
- Zhang GJ, Song X (2009) Interaction of deep and shallow convection is key to Madden–Julian oscillation simulation. *Geophys Res Lett* 36: 9708